Effect of simultaneous application of ultrasonic vibrations during laser surface melting on electrochemical properties of 2024 aluminum alloy

Sourabh Biswas, Sam Allison, S. Habib Alavi, and Sandip P. Harimkar*

School of Mechanical and Aerospace Engineering, Oklahoma State University, Stillwater, OK 74078, United States

*Corresponding author, Tel: +1(405)744-5830, E-mail: sandip.harimkar@okstate.edu

Received: 01 June 2017, Revised: 12 June 2017 and Accepted: 26 July 2017

DOI: 10.5185/amp.2017/043
www.vbripress.com/amp

Abstract

In the present investigation, effect of laser melting with and without simultaneous application of ultrasonic vibrations on electrochemical properties of 2024 aluminum alloy is investigated. The electrochemical behavior of the laser melted specimens was studied using open-circuit and potentiodynamic polarization measurements. Subsequently, investigation of the corrosion films was performed using scanning electron microscopy. It was observed that the laser melted specimens exhibited significant improvement in open circuit potential (both with and without simultaneous ultrasonic vibration application). The open circuit potential of the laser melted specimen without ultrasonic vibrations was observed to be more stable compared to the laser melted specimen with ultrasonic vibrations. It was observed that the corrosion mechanism undergoes a transition from pitting to uniform corrosion in the laser treated specimen, particularly in the laser melted specimen without ultrasonic vibrations. However, the extensive agitations due to ultrasonic vibrations in the melt pool appear to restrict Cu migration to grain boundaries that result in porous and relatively inefficient passive layer formation in laser processed samples with application of ultrasonic vibrations. This behavior was also observed in the potentiodynamic polarization studies that showed that the laser melted specimen without ultrasonic vibrations exhibited lower corrosion current and corrosion rate compared to the laser melted specimen with ultrasonic vibrations as well as the as received substrate.

Keywords: 2024 aluminum alloy, corrosion, laser melting, ultrasonic vibrations.

Introduction

Aluminum alloys have gained rapid popularity due to their excellent strength-to-weight ratio, warm formability, and corrosion resistance, making them one of the most extensively used materials in aerospace, automobile, and sport goods applications. Their corrosion resistance has often been attributed to the formation of highly conformal and corrosion resistant oxide layer rendering the alloy passive to electrochemical reactions. However, high strength aluminum alloys such as 2024 and 7075 have been reported to exhibit considerably inferior electrochemical properties due to presence of highly electropositive, and therefore, cathodic phases that trigger pitting on the surface. It has been reported that the pitting corrosion is particularly aggravated in chloride rich environments that reduce the stability of the oxide layer **[1]**. Hence, improvement of surface electrochemical properties of these alloys have been extensively studied using various surface engineering techniques such as anodizing **[2]**, electrodeposition **[3]**, and laser surface engineering techniques (laser surface alloying and laser surface melting) **[4, 5]**.

Among the aforementioned processes, non-equilibrium processing capabilities and very fast processing rates have made laser surface engineering one of the most extensively used techniques for improving corrosion resistance of aluminum alloys. For instance, an increase in open circuit potential (OCP) as well as transition of corrosion mechanism from intergranular to intragranular in laser processed 2024 aluminum alloy has been reported **[6]**. The observation was attributed to the dissolution of cathodic precipitates during the laser melting of the surface. Similarly, it has been reported that laser melted friction stir welds of 2024 aluminum alloy exhibit more electropositive behavior while large pitting was observed in the untreated zones **[7]**.

In the realm of solidification, the simultaneous application of ultrasonic vibrations during metal casting to achieve more refined microstructure, and thereby, superior mechanical and chemical properties has been widely studied **[8, 9]**. The ultrasonic vibrations have been successfully employed to achieve degassing **[10]**, superior corrosion resistance and tensile strength **[9]**, and elimination of unmixed zones during welding **[11]**. However, their effect on microstructure during very fast

solidification (usually associated with laser processing) has not been extensively reported. It has been reported that laser melting under the influence of ultrasonic vibrations results in significant microstructural refinement and improvement in surface hardness for Ti-6Al-4V alloy **[12]**. The present investigation is directed towards understanding the effect of ultrasonic vibration-assisted laser melting on the electrochemical properties of 2024 aluminum alloys.

Experimental

Materials

The substrate material used in the investigation was 2024 aluminum alloy.

Material processing

The laser processing experiments were performed using a set-up consisting of a continuous wave CO_2 laser (Ferranti) and a 750 W ultrasonic power supply with a 1 inch diameter titanium alloy probe (Sonics & Materials Inc.). Each aluminum alloy sample was mounted on the ultrasonic vibration probe that was fixed on a movable X-Y stage, as presented in **Fig. 1.** The surfaces of the samples were carefully polished using 2000 grit SiC paper and then sand blasted for 15 seconds to increase laser absorptivity. The ultrasonic vibration-assisted laser melting was performed with laser power of 950 W, ultrasonic vibration power output of 60% at vibration frequency of 20 kHz, and laser scanning speeds of 20 and 30 mm/s (corresponding to sample designations UL20 and UL30). For comparison, samples were also processed with the similar laser processing parameters i.e. laser power of 950 W and scanning speeds of 20 mm/s and 30 mm/s without simultaneous application of ultrasonic vibrations (sample designations U20 and U30). The summary of the experimental parameters for laser melting with and without simultaneous application of ultrasonic vibrations is given in **Table 1**.

Table 1. Processing parameters for laser melting of 2024 alloy without and with the simultaneous application of ultrasonic vibrations.

Sample	Power (W)	Working Distance (mm)	Scanning Speed (mm/s)	Ultrasonic Amplitude (%)
L20	950	5	20	-
L30	950	5	30	-
UL20	950	5	20	60%
UL30	950	5	30	60%

Characterizations

The open circuit and potentiodynamic polarization measurements were performed in naturally aerated 3.5% NaCl solution using a potentiostat/galvanostat (Ametek Scientific Instruments). The potentiostatic experiments were performed for 20,000 s and the corrosion films were subsequently characterized using a scanning electron microscopy (FEI Quanta 600). The potentiodynamic experiments were performed by scanning the current response from -0.25 V to +0.25 V with respect to the open circuit potential at a sweep rate of 0.33 mV/s.

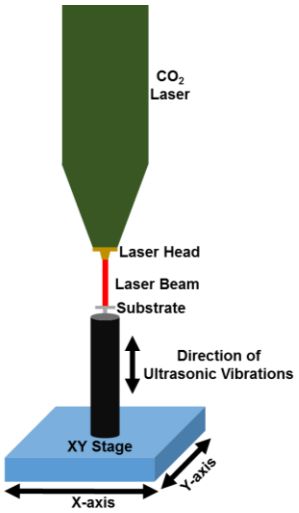

Fig. 1. Schematic diagram of the apparatus used for conducting the laser melting experiments with and without the simultaneous application of ultrasonic vibrations.

Results and discussion

Open circuit corrosion behavior

The open circuit corrosion data of the as received, laser surface melted 2024 aluminum alloy with and without the simultaneous influence of ultrasonic vibrations is presented in **Fig. 2**. The as received material exhibited very stable open circuit potential of about -590 mV in the initial stage (<15,000s) followed by slight decrease to about -610 mV. Such observation is common for aluminum based alloys that exhibit initial increase in open circuit potential due to formation of passive oxide (Al_2O_3) layer and eventual exfoliation of the film in the later stages due to pitting **[13]**. In comparison, the laser melted specimens both with (UL20 and UL30) and without (L20 and L30) simultaneous application of ultrasonic vibrations showed significant increase in corresponding open circuit potential to about -470 to -490 mV in the initial stages. It has been reported that the rapid resolidification after laser melting results in considerable elemental redistribution, particularly segregation of Cu along the grain boundaries, that renders the grain boundaries more electropositive as compared to the grain bodies **[6, 7]**. The laser melted specimens without simultaneous application of ultrasonic vibrations (L20 and L30) manifested not only higher open circuit potential but also relatively stable potential. The open circuit potential of the L20 and L30 specimens decreased from about -475 mV to -515 mV. Such a stable open circuit potential of laser melted specimens can be attributed to higher relative stability of the passive oxide film without the destabilizing effects from the electropositive precipitates that promote pitting.

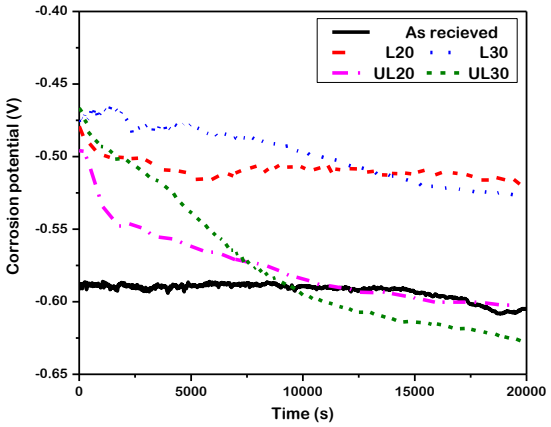

Fig. 2. Variation of open circuit potential with time for as received and laser melted 2024 aluminum alloy with and without application of ultrasonic vibrations.

Compared to laser melted specimens, the alloys laser melted with simultaneous application of ultrasonic vibrations (UL20 and UL30) exhibited notable decrease in open circuit potential with time (**Fig. 2**). The open circuit potential decreased from -473 mV to -630 mV and -500 mV to -604 mV over 20,000 s for UL20 and UL 30 specimens, respectively. Since the variation in open circuit potential is often directly related with the stability of corrosion films, it can be inferred that the passive layer formation for specimens laser melted with simultaneous application of ultrasonic vibrations (UL20 and UL30) was not very efficient compared to L20 and L30 specimens. Hence, subsequent efforts were directed primarily in the characterization of the corrosion film using microstructural techniques.

Microstructural characterization

Surface microstructures of as received and laser melted 2024 aluminum alloy with and without simultaneous application of ultrasonic vibrations after immersing for 20,000s are presented in **Fig. 3**. It can be clearly observed that as received specimens exhibit pitting characteristics with extensive corrosion products on the surface (**Fig. 3a**). It has been widely accepted that the passive oxide layer in aluminum alloys is primarily composed of aluminum oxide formed according to reaction **[14]**:

$$2Al + 6H_2O \rightarrow Al_2O_3.3H_2O\ (\text{bayerite}) + 3H_2$$

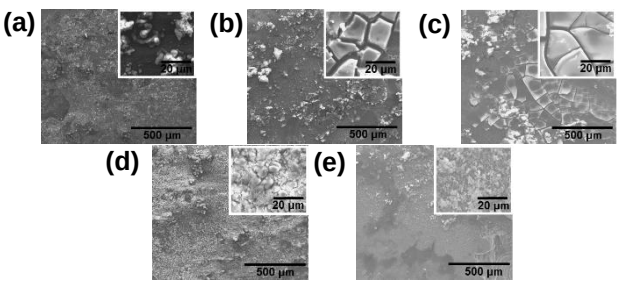

Fig. 3. Microstructures of corroded surfaces for (a) as received, (b) L20, (c) L30, (d) UL20, and (e) UL30 specimens (higher magnification images are provided in the insets).

The laser melted specimens without simultaneous application of ultrasonic vibrations (L20 and L30) exhibited highly plate like features for the surface oxide layer (**Fig. 3b-c**). The formation of such conformal oxide layer with polygonal plate-like features is a characteristic of microgalvanic uniform corrosion **[15]**. It also indicates that the oxide layer most likely nucleated from the bulk of the grains (compared to the grain boundaries that were cathodic due to copper migration) and was a relatively stable formation process. In comparison, the specimens laser melted with simultaneous application of ultrasonic vibrations (UL20 and UL30) exhibited a corrosion mechanism highly similar to the as received specimen with porous and uneven corrosion surface (**Fig. 3. d-e**). It appears that even the passive layer formation was not very continuous in the UL20 and UL30 specimens that resulted in the aforementioned morphology of the corrosion film. It can be inferred that while the laser melting under the influence of ultrasonic vibrations resulted in partial elimination of the precipitates, the extensive turbulence in the melt due to ultrasonic vibrations restricted the complete migration of the Cu atoms towards the grain boundaries and the atoms most likely remained segregated in the grains. This observation is in good agreement with the initial passivation and eventual decay of the open circuit potential of the UL20 and UL30 specimens in the potentiostatic experiments.

Potentiodynamic polarization measurements

The potentiodynamic polarization curves for as received and laser melted 2024 aluminum alloy with and without simultaneous application of ultrasonic vibrations are presented in **Fig. 4**. The presence of single polarization line in each of the scans clearly indicate that the polarization current is controlled exclusively by charge transfer across the electrode-electrolyte interface **[16]**. Also, very similar to the observations from the potentiostatic results, it can be clearly observed that laser melting resulted in considerable improvement in corrosion potential, E_{corr} (**Table 2**). The specimens laser melted without simultaneous application of ultrasonic vibrations also showed an improvement in corrosion resistance (based corrosion current, I_{corr}, and corrosion rate calculated from Faraday's law).

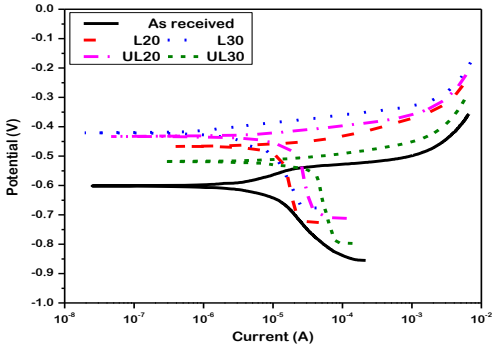

Fig. 4. Potentiodynamic polarization curves for as received and laser melted 2024 aluminum alloy with and without simultaneous application of ultrasonic vibrations.

The application of ultrasonic vibrations during laser melting apparently resulted in slight deterioration of corrosion resistance compared to both as received and as laser melted specimens.

Table 2. The results of potentiodynamic polarization tests on laser melted 2024 aluminum alloy with and without application of ultrasonic vibrations.

Sample	E_{corr} (mV)	I_{corr} ($\mu A/cm^2$)	Corrosion rate (μm/y)
As Received	-601	2.875	4.56
L20	-465	2.575	4.08
L30	-409	1.248	1.98
UL20	-427	5.244	8.32
UL30	-526	9.438	14.97

Conclusion

In this investigation, laser melting of 2024 aluminum alloy specimens with and without application of simultaneous of ultrasonic vibrations was successfully performed. The laser melted specimen without ultrasonic vibrations exhibited increase in open-circuit potential (higher corrosion potential) as well as decrease in corrosion rate compared to the specimens laser melted with ultrasonic vibrations. The laser melted specimen with ultrasonic vibrations exhibited an initial improvement in open-circuit potential, however, their open circuit potential underwent rapid decrease that was confirmed to be a consequence of decreased stability of the passive corrosion film.

Acknowledgements

This material is based upon work supported by the National Science Foundation under Grant No. CMMI- 1149079.

Author's contributions

Conceived the plan: SB, SPH; Performed the expeirments: SB, SA, SHA; Data analysis: SB; Wrote the paper: SB, SHA, SPH. Authors have no competing financial interests.

References

1. Foley, R.T.; Corrosion, **1986,** *42, 277.* **DOI:** http://dx.doi.org/10.5006/1.3584905
2. Huang, Y.; Shih H.; Huang, H.; Daugherty, J.; Wu, S.; Ramanathan, S.; Chang, C.; Mansfeld, F., Corros. Sci., **2008,** *50, 3569.* **DOI:** http://doi.org/10.1016/j.corsci.2008.09.008
3. Hu, J.M.; Liu, L.; Zhang J.Q.; C.N. Cao, Prog. Org. Coat., **2007**, *58, 265*. http://doi.org/10.1016/j.porgcoat.2006.11.008
4. Watkins, K.G.; McMahon, M.A.; Steen, W.M., Mater. Sci. Eng., A, **1997**, *231, 55.* **DOI:** http://doi.org/10.1016/S0921-5093(97)00034-8
5. Yue, T.M.; Yan, L.J.; Chan, C.P.; Dong, C.F.; Man H.C.; Pang, G.K.H., Surf. Coat. Technol., **2004**, *179, 158*. **DOI:** http://doi.org/10.1016/S0257-8972(03)00850-8
6. Li, R., Ferreira; M.G.S., Almeida; A., Vilar, R.; Watkins, K.G.; McMahon, M.A.; Steen, W.M.; Surf. Coat. Technol.., **1996**, *81, 290*. **DOI:** https://doi.org/10.1016/0257-8972(95)02484-0
7. Kalita, S.J., Appl. Surf. Sci., **2011**, *257, 3985*. **DOI:** http://doi.org/10.1016/j.apsusc.2010.11.163
8. Liu, X.; Osawa, Y.; Takamori, S.; Mukai, T., Mater. Sci. Eng., A, **2008**, *487, 120*. **DOI:** http://doi.org/10.1016/j.msea.2007.09.071
9. Yao, L.; Hao, H.; Ji, S.H.; Fang, C.F.; Zhang, X.G., Trans. Nonferrous Met. Soc. China, **2011**, *21, 1241*. **DOI:** https://doi.org/10.1016/S1003-6326(11)60848-0
10. Xu, H.; Jian, X.; Meek, T.T.; Han, Q.; Mater. Lett., **2004**, *58, 3669*. **DOI:** http://doi.org/10.1016/j.matlet.2004.02.055
11. Cui, Y. Xu, C.L., Han, Q., Scr. Mater., **2006,** *55, 975*. **DOI:** http://doi.org/10.1016/j.scriptamat.2006.08.035
12. Biswas S.; Habib Alavi S.; Harimkar S.P., Mater. Lett., **2015**, *159, 470*. **DOI:** http://doi.org/10.1016/j.matlet.2015.07.059
13. Polmear, I.J. (3rd Eds.); Light alloys : metallurgy of the light metals, Oxford: Butterworth-Heinemann, **2000**.
14. Davis, J.R. (2nd Eds.); Corrosion of aluminum and aluminum alloys, Materials Park: ASM International, **1999**.
15. Pardo A.; Merino, M.C.; Coy, A.E.; Arrabal, R.; Viejo, F.; Matykina, E.; Corros. Sci., **2008,** *50, 823*. **DOI:** https://doi.org/10.1016/j.corsci.2007.11.005
16. Mandal, M.; Moon, A.P.; Deo, G.; Mendis, C.L.; Mondal K., Corros. Sci., **2014,** *78, 172*. **DOI:** https://doi.org/10.1016/j.corsci.2013.09.012

